

LASER INTERFEROMETER GRAVITATIONAL WAVE OBSERVATORY
- LIGO -
CALIFORNIA INSTITUTE OF TECHNOLOGY
MASSACHUSETTS INSTITUTE OF TECHNOLOGY

Technical report LIGO-T980121-00 - V 12/17/98

**Preliminary results from Livingston VE
vibration & acoustic testing**

M. Zucker, K. Martini*

*Cambridge Acoustical Associates, Cambridge, MA

Distribution of this draft:

All interested.

*Note: This document is incomprehensible in black and white.
We apologize for any inconvenience..*

This is an internal working note
of the LIGO Project.

California Institute of Technology
LIGO Project - MS 51-33
Pasadena CA 91125
Phone (818) 395-2129
Fax (818) 304-9834
E-mail: info@ligo.caltech.edu

Massachusetts Institute of Technology
LIGO Project - MS 20B-145
Cambridge, MA 01239
Phone (617) 253-4824
Fax (617) 253-7014
E-mail: info@ligo.mit.edu

WWW: <http://www.ligo.caltech.edu/>

1 INTRODUCTION

From 12/4 through 12/7/98, Kyle Martini of Cambridge Acoustical Associates (CAA) conducted vibration and acoustic testing of the LIGO Vacuum Equipment at the Livingston site, under contract from Process Systems International (PSI). M. Zucker monitored and assisted these tests, which are primarily designed to evaluate structural and acoustic noise introduced by equipment provided by PSI, and to identify transmission paths for this noise to sensitive points of the LIGO detector.

The main contractual pass/fail criterion under consideration is the induced shock at detector mounting locations caused by actuation of PSI-supplied gate valves. Most other aspects of the PSI noise mitigation effort were undertaken on a “best effort” basis, and the evaluation is thus mostly informational. Results of the valve shock tests, and a more thorough analysis of the complete suite of measurements, will be provided by CAA in a forthcoming report. However, as in previous tests conducted at the Hanford site, MZ monitored up to two data channels (chosen from the eight simultaneously recorded by CAA) using a standalone HP 35670A dynamic signal analyzer and an oscilloscope. We used these two channels as a “quick-look” window to scrutinize particularly interesting features of the vacuum equipment and its facility environment. Some results gleaned from this narrow slice through the test data are presented here for general information and, we hope, to stimulate further studies.

2 APPARATUS

To avoid noise contamination generated by the measurement equipment fans and disk drives we located all the instrumentation in the LVEA or VEA major equipment access vestibule (“wash bay”) and ran signal and power cables under the closed rollup door isolating this area from the LVEA/VEA. The sensors are summarized in Table 1 and their setup is shown in Figure . Each sensor’s filter or preamp was located on the floor near the sensor mounting position, and connected by up to 200 feet of RG-58 coax cable to the measuring station.

For low-level accelerations and sound we used seven Wilcoxon 741A accelerometers¹ and a Bruel and Kjaer 2236 sound level meter, respectively. The accelerometers were all joined to their matched Wilcoxon P31 battery-operated preamplifiers using twinax cables provided by the manufacturer. At one point we placed all seven of the 741A’s on the floor near one another and verified that they all gave similar outputs; we subsequently assumed they were all in compliance with their individual factory calibration certs (which vary by about $\pm 10\%$ from the nominal 1000 V/g from unit to unit; we just use the nominal value for data presented here). Three of the seven were new and previously unused.

The sound level meter provides an analog output which was filtered and amplified by a Frequency Devices 901 filter before being digitized. It was calibrated using a portable B&K microphone calibrator, which emits a 1 kHz sinusoidal tone into a small cavity sealed around the microphone barrel at a pressure of 1 Pa RMS (+94 dB with respect to 20 μ Pa RMS). To use this calibrator without distortion, the microphone preamp gain had to be temporarily reduced by 20 dB and the

1. For valve shock, less sensitive and more robust accelerometers were used.

filter corner frequency increased to 5 kHz. The 20 dB correction was then included in the calibration factor.

The HP 35670A spectrum analyzer was set to a DC-400 Hz frequency range, with Hanning window function and frequency resolution of either 800 lines (0.75 Hz noise bandwidth) or 1600 lines (0.375 Hz noise bandwidth). Data presented below have been corrected for bandwidth and presented as spectral densities. For each test we verified that the analyzer front end noise was at least 15 dB below the measured noise level, thus contributing $< 3\%$ error to the measured voltage spectral density in any bin. Traces were saved in ASCII format on floppy disks, which were transferred to a laptop computer for display and analysis. Screenshot images were also plotted out directly on a printer for archival and logging purposes.

<i>sensor</i>	<i>preamp/filter</i>	<i>freq range</i>	<i>sensitivity</i>	<i>noise RTI</i>
Wilcoxon 741A	Wilcoxon P31	.01 - 450 Hz	1000 V/g	$1 \times 10^{-8} \text{ g}/\sqrt{\text{Hz}}$
B&K 2236	Frequency Devices 901	10 - 500 Hz	2.2 V / Pa	$3 \times 10^{-5} \text{ Pa}/\sqrt{\text{Hz}}$

Table 1: Instrumentation parameters for these tests

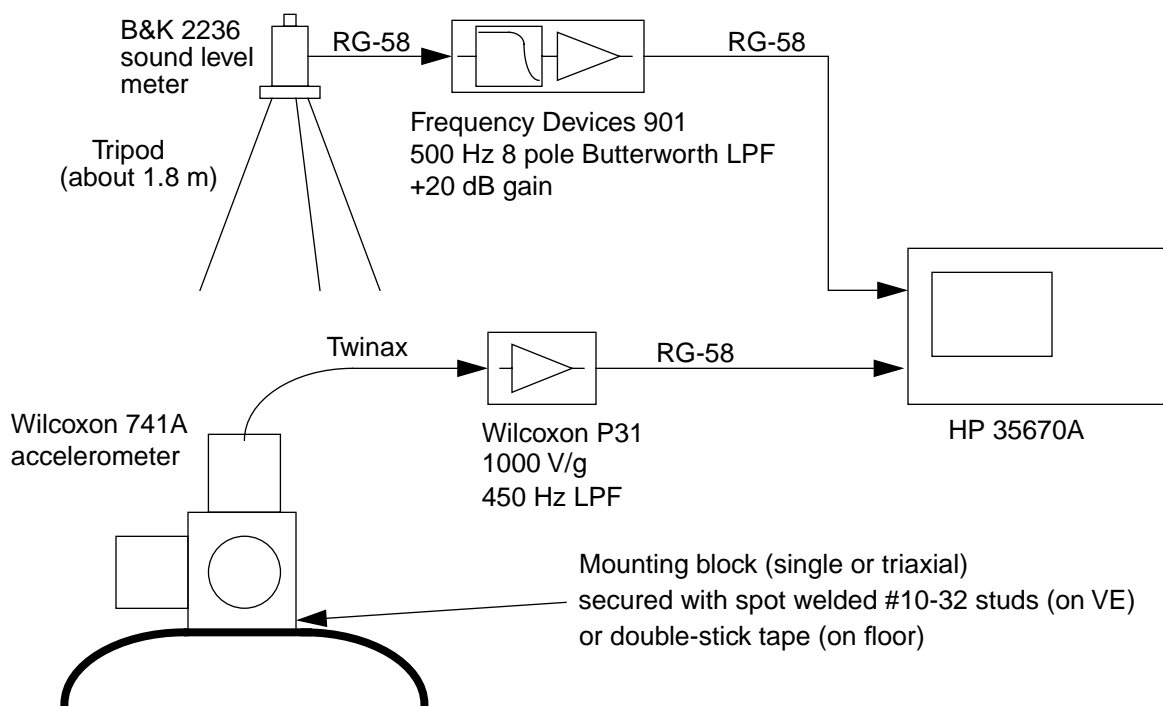


Figure 1: Accelerometer and microphone setup

3 LEFT (Y) END STATION TESTS

In the Y end station we designated one accelerometer on the floor, near the southeast leg of the BSC chamber, as our “reference” accelerometer. The other six accelerometers were deployed in several different configurations, e.g., on the center NE “G” nozzle of the BSC, on manifold flanges and stiffeners, on the middle stiffener of the short cryopump, and on the SE support leg of the BSC about 20 cm above floor height. To mount the accelerometers on the vacuum envelope we spot-welded #10-32 stainless steel studs to wall or flange surfaces and thereby bolted an accelerometer mounting block directly to the chamber. Two types of block were used, a triaxial cube (made by Wilcoxon to hold three 741A’s at mutual right angles) or a flat uniaxial plate (home-made). Each accelerometer was then attached to its block with a single 3/8-16 set screw and hand tightened. We placed the microphone about 1 meter east of the east 60” door on the BSC chamber.

To determine background levels we measured sound and vibration with the facility air conditioning system as we found it, and then turned off the following equipment;

- All HVAC fans (breakers in the mechanical room)
- Facility chilled water circulation pumps (in outdoor chiller yard)
- Facility chiller units (in chiller yard)
- Facility air compressors (in chiller yard).

Winds were light and no rain fell during the actual data accumulations. We left the VE controls rack, its Sun computer and monitor, and its fancooled VME crate running the whole time since turning them off was deemed risky. We did install and secure the side and back panels on the rack and shut the door. Foam packing material was stuffed in the pipe passthrough from the mechanical room into the VEA to simulate the lagging which will eventually be added here after the PSI equipment has been accepted.

Figure 5 shows the acoustic spectrum in the maximally quiet “background” state and with the facility air conditioning (and chilled water) operating normally.

After evaluating the background condition we then operated the PSI turbomolecular pump, which was attached to the 10” manifold pumpout flange. We also ran its backing pump and the PSI chilled water booster pump in the mechanical room. Although the facility CW system was off, the large stored volume and small heat load from the two PSI pumps allows them to operate for extended periods with just their booster.

Figure 2 and Figure 3 show the vertical floor acceleration near the BSC chamber in each of these conditions. For comparison, the so-called “LIGO Standard Spectrum” for ground motion (LSS) is plotted as well¹. Note that the vibration induced by the turbopump/backing pump operation is in most cases below that induced by the facility air conditioning. From previous tests we believe the main source of broadband noise associated with the turbopump is actually its QDP80 backing

1. Defined as displacement spectral density $X_{LSS} = 10^{-9} \text{ m}/\sqrt{\text{Hz}} \times (1 \text{ Hz}/f)^3$ from 0 to 1 Hz, $X_{LSS} = 10^{-9} \text{ m}/\sqrt{\text{Hz}}$ from 1 Hz to 10 Hz, and $X_{LSS} = 10^{-9} \text{ m}/\sqrt{\text{Hz}} \times (10 \text{ Hz}/f)^2$ above 10 Hz. This corresponds to an acceleration $A_{LSS} = 0.4 \mu\text{g}/\sqrt{\text{Hz}}$ above 10 Hz.

pump located in the mechanical room. There are also “line” features from the turbo rotation at its fundamental and harmonics; these are off scale in the data shown (above 400 Hz).

Figure 4 shows the radial (horizontal) vibration of the middle G nozzle on the northeast side of the BSC with all quiet and with the turbo, backing pump and chilled water booster running. As expected the effect of the turbo is more dramatic on the vacuum envelope, although it is not clear whether the enhanced vibration is structure-borne or acoustically excited.

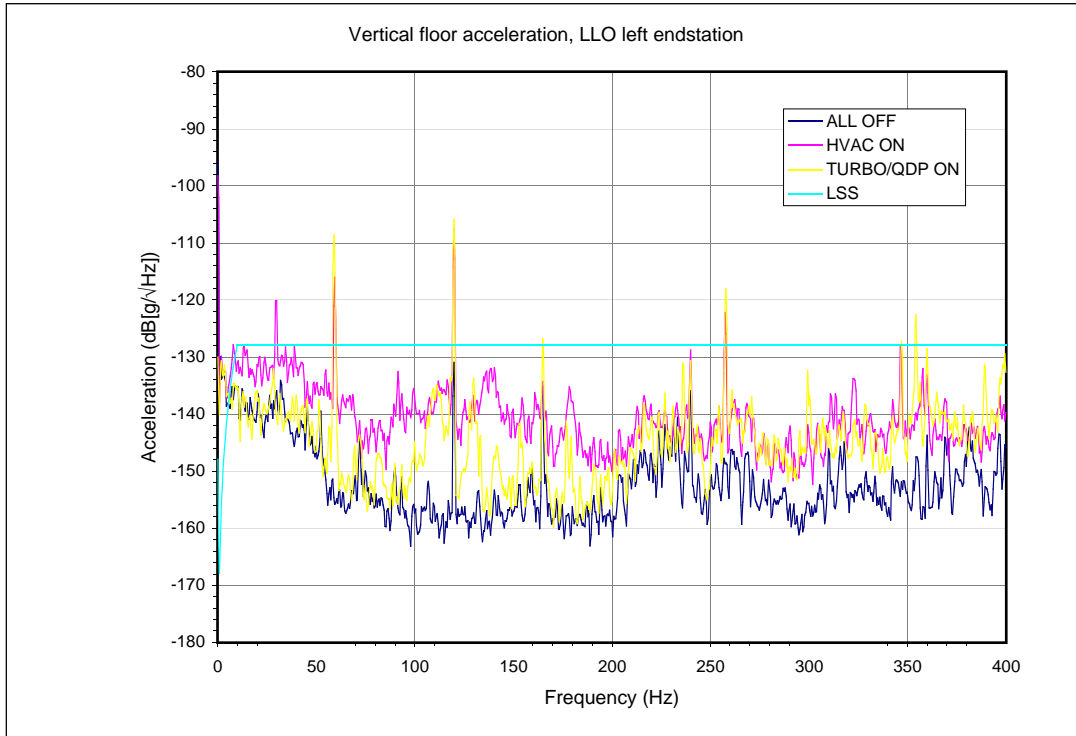


Figure 2: Vertical acceleration of LLO left endstation floor near BSC.

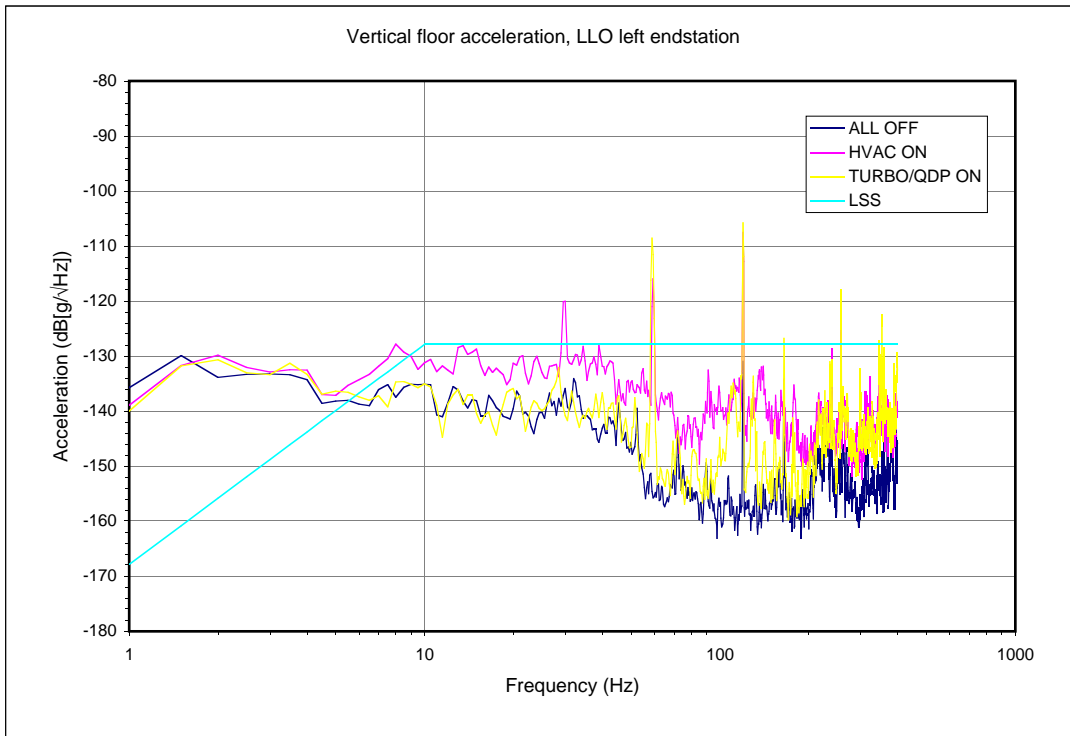


Figure 3: Data of Figure 2 plotted with logarithmic frequency scale.

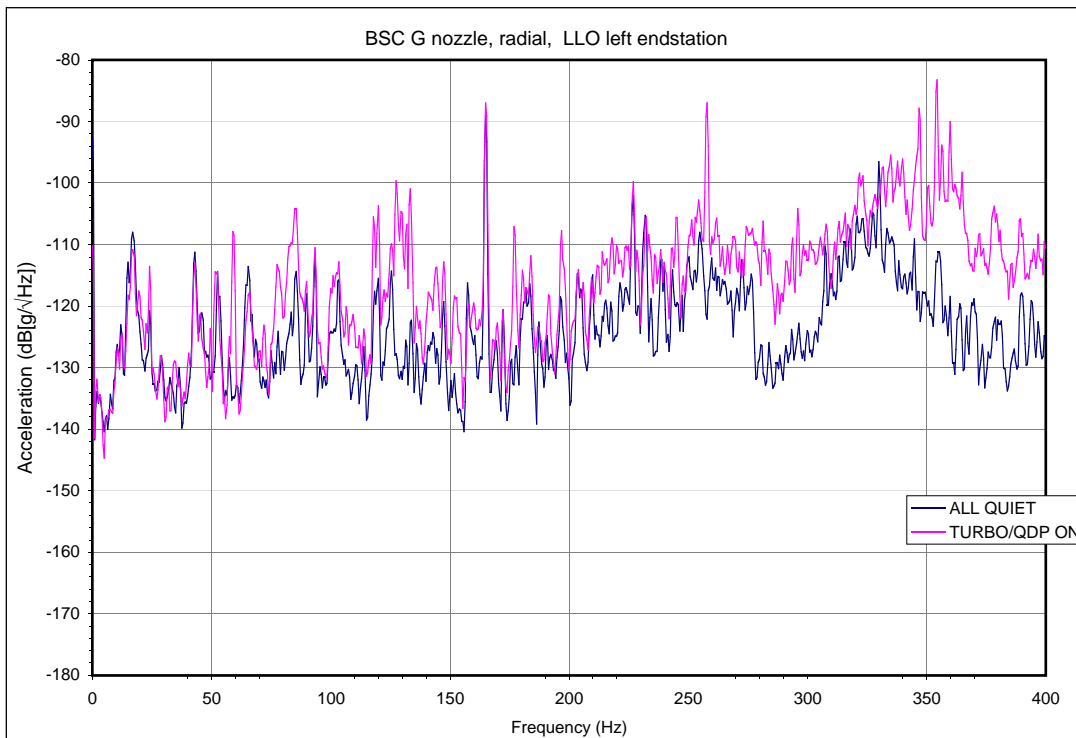


Figure 4: Effect of turbopump and backing pump on BSC wall vibration.

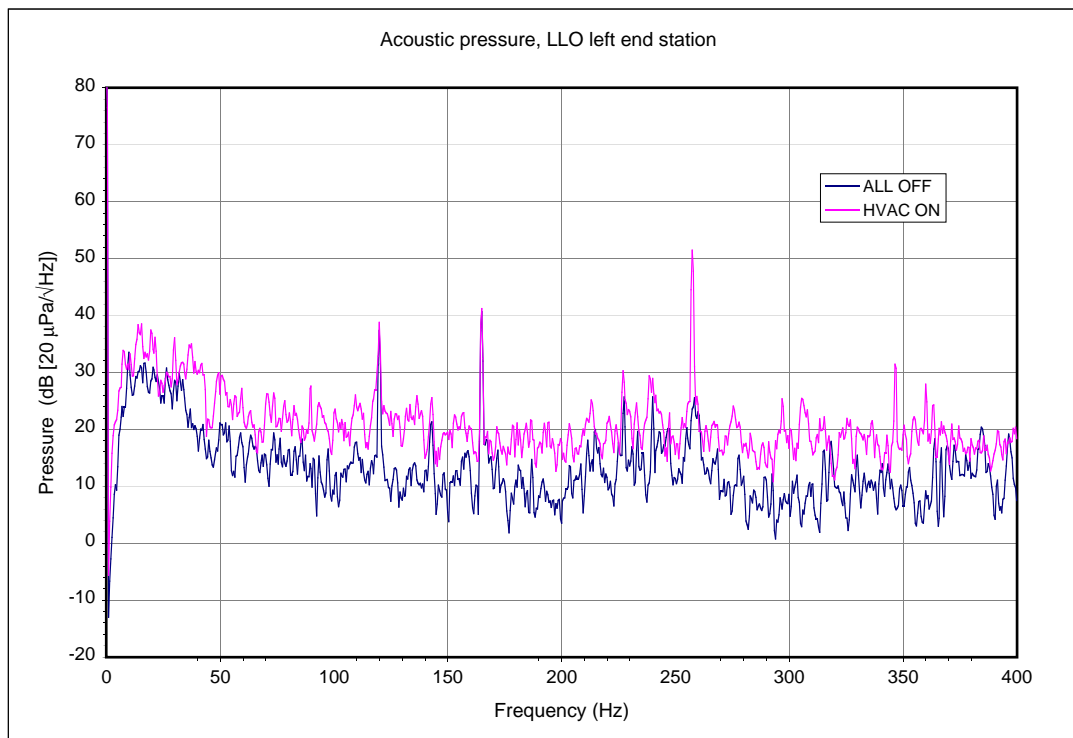


Figure 5: Microphone in quiet conditions and with facility HVAC turned on (including chillers and circulating pumps).

The final test in the Y end station looked for excess noise due to bubbling or flowing of fluid or gas in the LN2 cryopump. Figure 6 shows the radial vibration of the cryo shell stiffener on 12/4, with all facility and PSI equipment turned off. The cryo was filled with liquid nitrogen immediately after this and allowed to stabilize over night. Using the control computer interface, the level control valve was adjusted by trial and error to provide a fixed continuous flow rate which almost identically cancelled the evaporative liquid loss. This was done to simulate the action of a continuous PID level control loop. In prior tests at Hanford, we found the vibration was nonstationary, with a significant increase just after each discrete transition of the level control valve. These are typical with the current “bang-bang” deadband level control algorithm. With the operating control bypassed in this way, the noise measured here appeared stationary. Although the “operating” data were taken a full day after the “warm” background, the floor vibration appeared to be about the same. At some frequencies, the cryo shell is a factor of 10 noisier in the operating state.

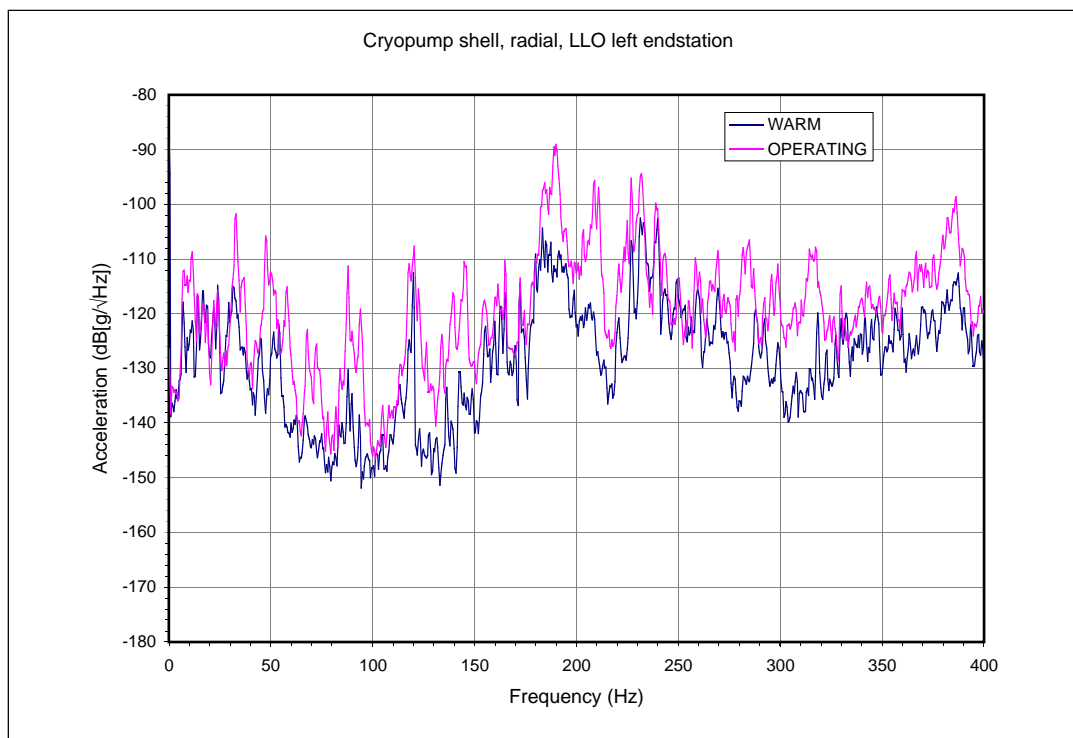


Figure 6: Radial acceleration of short cryopump stiffener, LLO left end station. The blue spectrum was taken 12/4 with the cryo empty and warm. Magenta trace is from late 12/5, after filling and stabilizing the cryo level.

4 CORNER STATION TESTS

In the corner we initially established the same kind of “all quiet” background as at the end station (Figure 7 and Figure 7). The floor “reference” accelerometer and the microphone were in this case located on the west side of LBSC3. In this case we separately manipulated the HVAC air handlers and the facility chillers and chilled water pumps located in the outdoor chiller yard. As can be seen in Figure 7 there was an excess caused by the chilled water system alone, especially at frequencies between 4 and 100 Hz. The air handlers remain the dominant contribution, however. Once again, we left the VE controls racks and their Sun computers running, although we insured that the rack side panels were installed and secured.

Toward the end of the tests we discovered that the wastewater treatment plant on the east side of the corner station was subject to cycling on and off on a timer; this could have affected some measurements. It did not appear to significantly affect the floor vibration at LBSC3, but may have generated acoustics (it was audible inside the station near the southeast corner) and thus vacuum envelope vibration.

Only the backing pump (QDP80) from one of the corner station turbopump sets was available at the time of testing. Since noise from the turbo itself had been characterized by CAA before, we

took this as an opportunity to gauge sound and vibration transmission from the mechanical room (where the QDP80 is located) into the LVEA floor and vacuum envelope. In this case we took no pains to block the wall opening which passes pipes and conduits from the mechanical room into the LVEA, so there was a fairly obvious acoustic path. Figure 9 shows the vibration level resulting from the QDP80 and the PSI chilled water booster pump on the LVEA floor vibration. Figure 10 shows the acoustic spectrum taken with the QDP 80 and the booster running, and with various combinations of facility equipment. In one instance we turned on only the HVAC fans without the chilled water. Surprisingly, this apparently produced higher noise than found with the full system running. It is possible that some fans which had not actually run in normal operation went on when the chillers were off (e.g., to deal with the increased apparent “load”). We did not investigate further, but it would be worthwhile in future to monitor the facility noise over a longer period to correlate changes in the spectrum with equipment cycles.

As in the end station, facility (HVAC) operation significantly elevates ambient sound pressure level, floor vibration and vacuum envelope vibration. As shown in Figure 11, over a fairly broad frequency range¹ the “operating:off” ratio is nearly the same for sound as for acceleration, e.g. about 10:1 for HVAC-induced noise near 50 Hz. We were thus tempted to try and map out the transmission paths by plotting linear transfer functions between acoustic and structural sensors, and assembled an array of 4 microphones and 7 accelerometers in the corner station.

However, the cross-spectral transfer functions measured between microphone and accelerometer pairs in the presence of HVAC noise (Figure 12) were significantly less than the anticipated ratio of the two spectral densities, and the cross-spectral coherence function (Figure 13) was insignificant except at isolated frequencies². This result was independent of frequency resolution (from 0.25 Hz to 1 Hz) and number of averages (from 8 to over 40). We conclude that, while the HVAC system clearly is a common source of both acoustic and structure-borne energy, the transfer function linking these two manifestations must be nonlinear, nonstationary, or possibly both.

By playing white noise through a small loudspeaker placed about 3 m from the microphone and floor accelerometer, we could also increase both acoustic and vibration levels above their respective backgrounds, but in this case the expected coherence was seen between them. It is therefore most likely that the acoustic-to-vibration transfer mechanism for HVAC-generated noise is non-stationary. One plausible scenario is that pockets of turbulence travel through air ducts and the room, thus continuously varying the relative delay between local acoustic pressure and the structural response at a given receiver location. This conjecture can be tested by measuring the correlation between sound field measurements at successively greater receiver separations.

-
1. which roughly corresponds to the frequency band where both sensor types have adequate SNR with respect to their electronic noise, in the quieter condition.
 2. Poor cross-spectral coherence was also typical for the vacuum pump-generated excess noise, although in this case the “operating:off” ratios are not so great and the expected coherence would thus be lower.

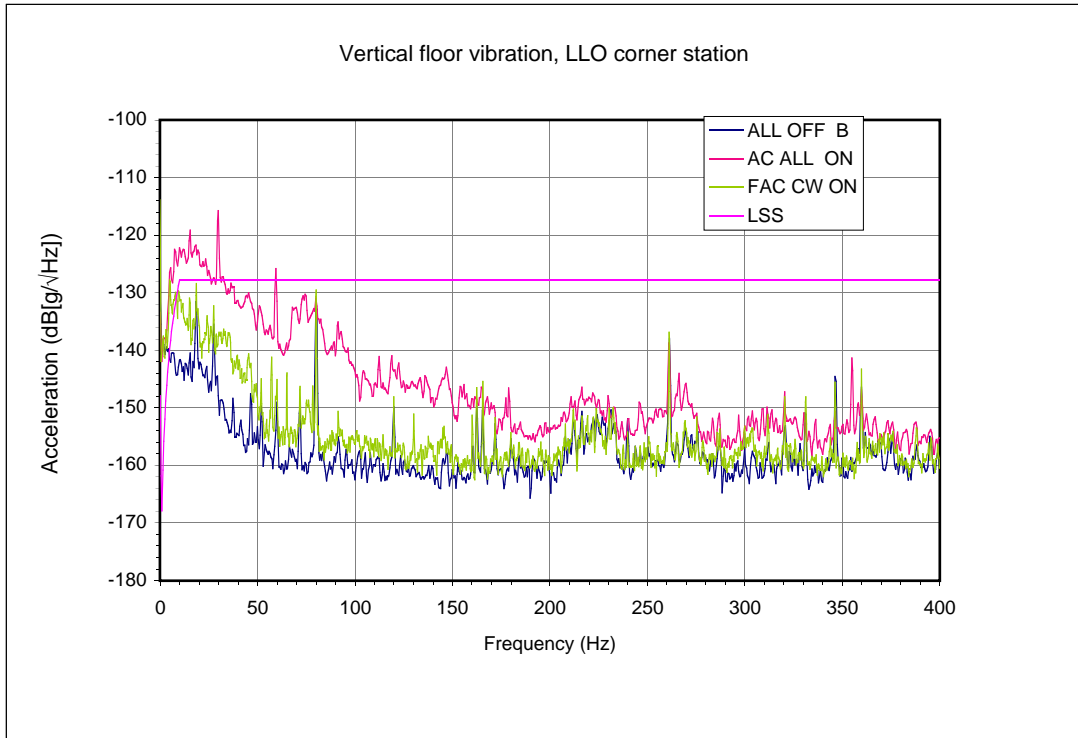


Figure 7: Vertical floor vibration, Livingston LVEA.

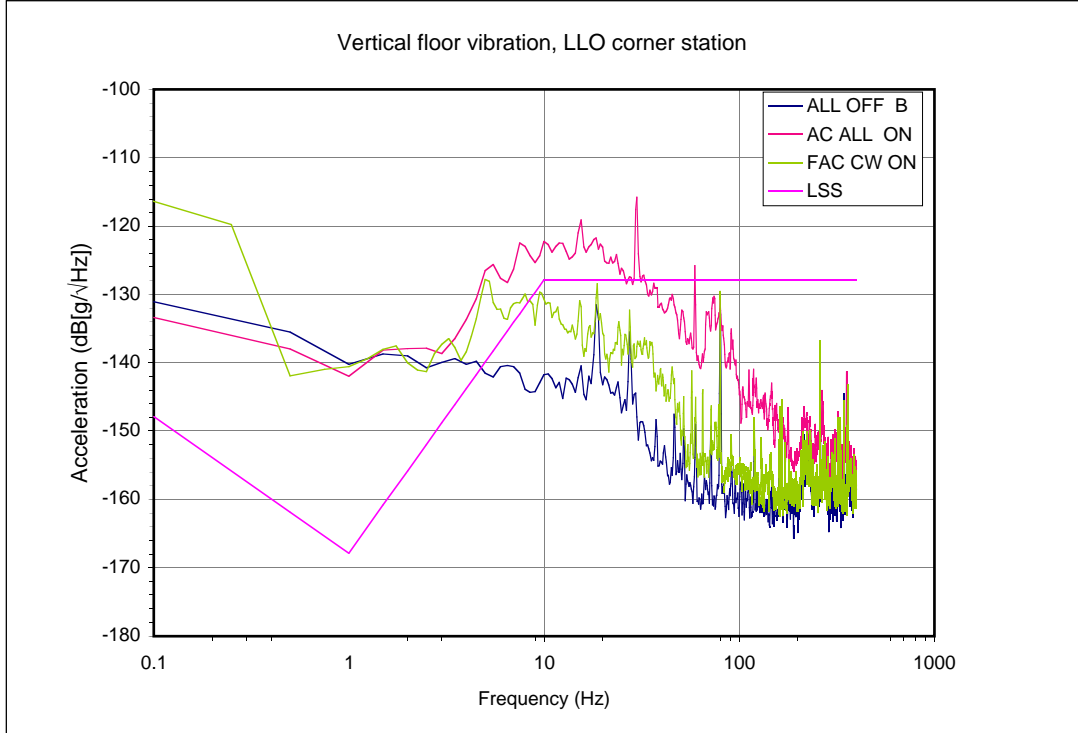


Figure 8: Data of Figure 7 plotted with log frequency scale.

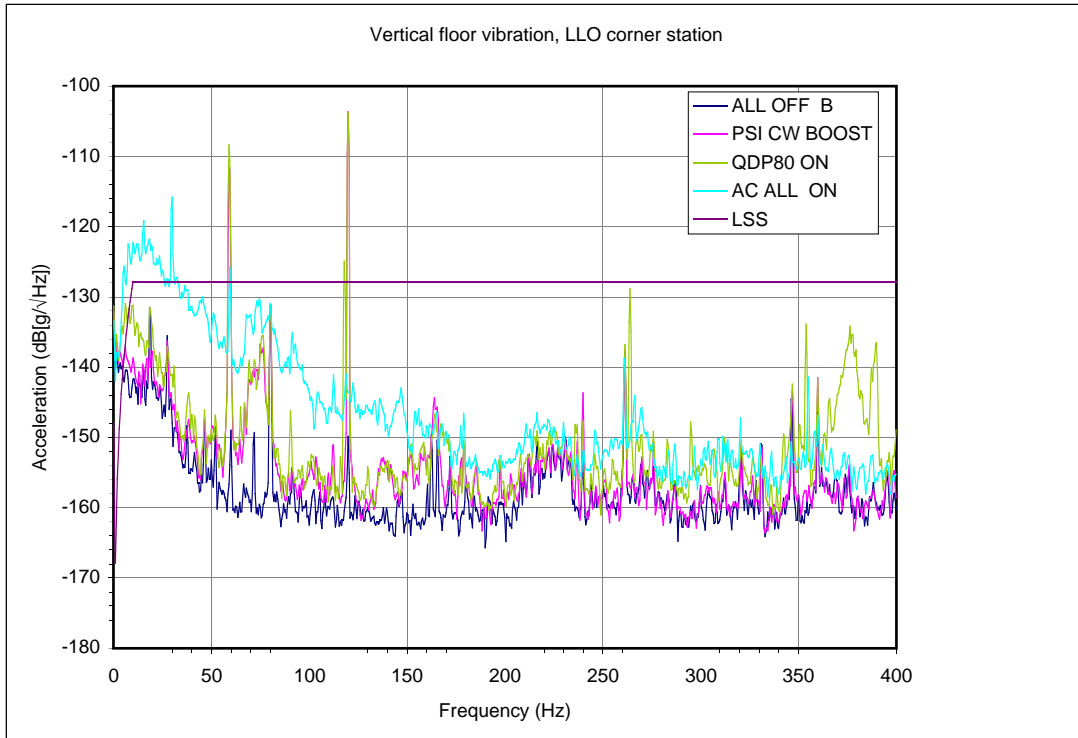


Figure 9: Vertical floor vibration vs. PSI equipment and HVAC on/off.

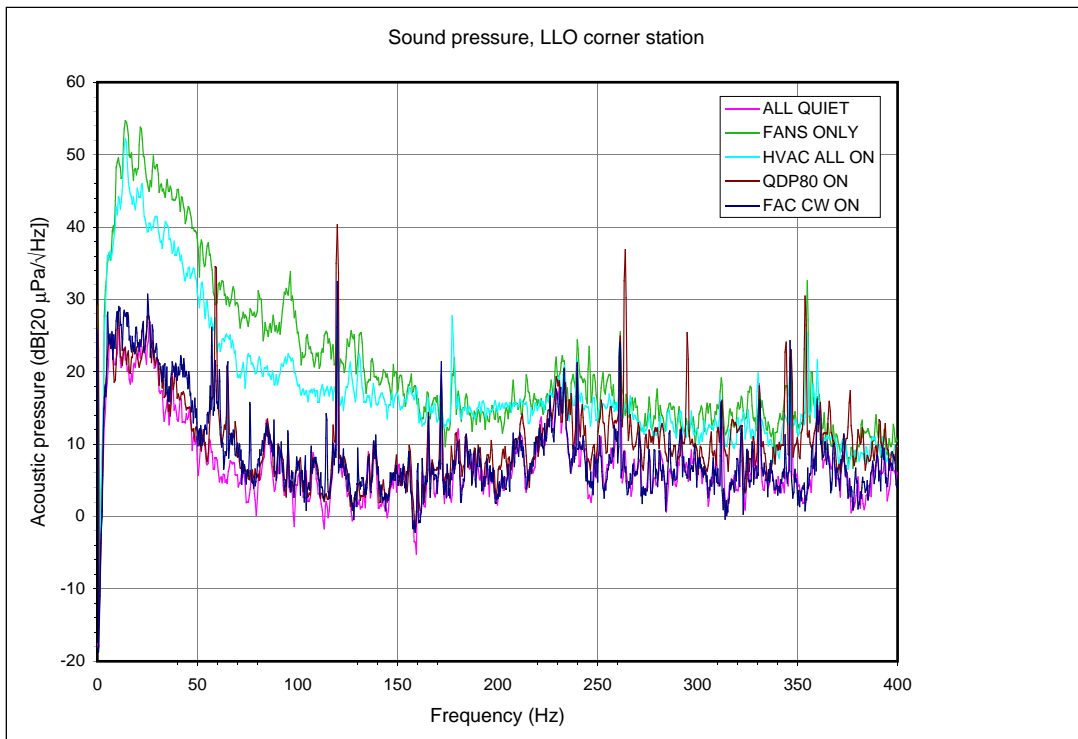


Figure 10: LVEA sound pressure vs. HVAC and PSI backing pump on/off.

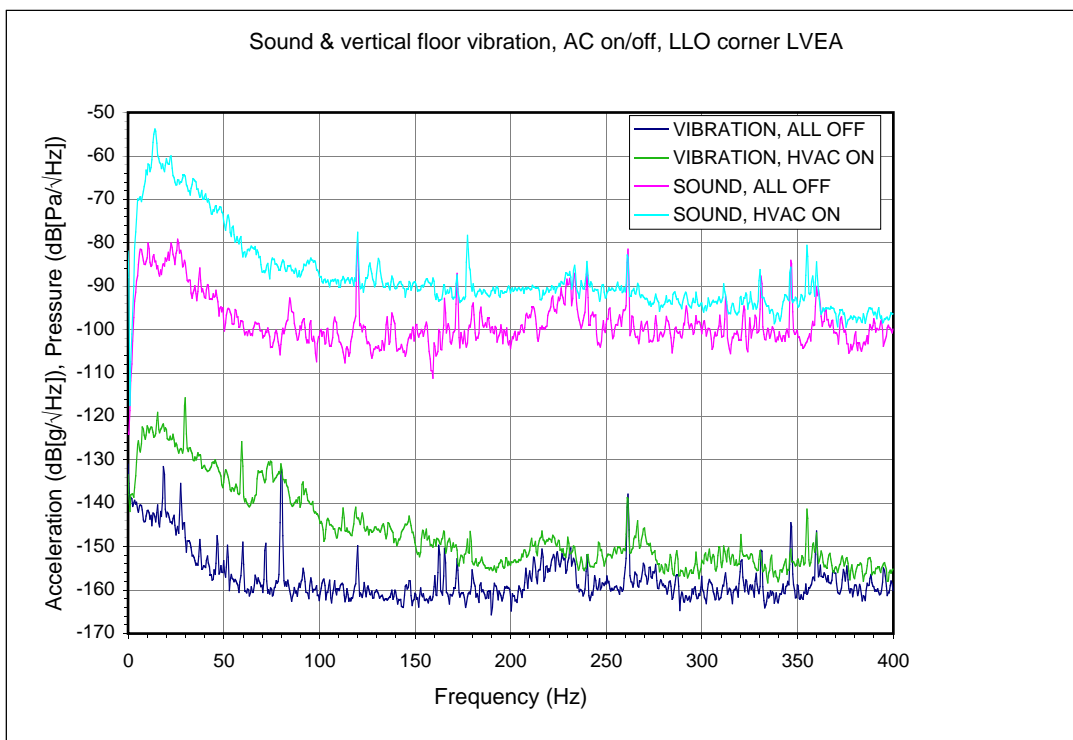


Figure 11: Change in LVEA floor vibration and sound pressure due to HVAC.

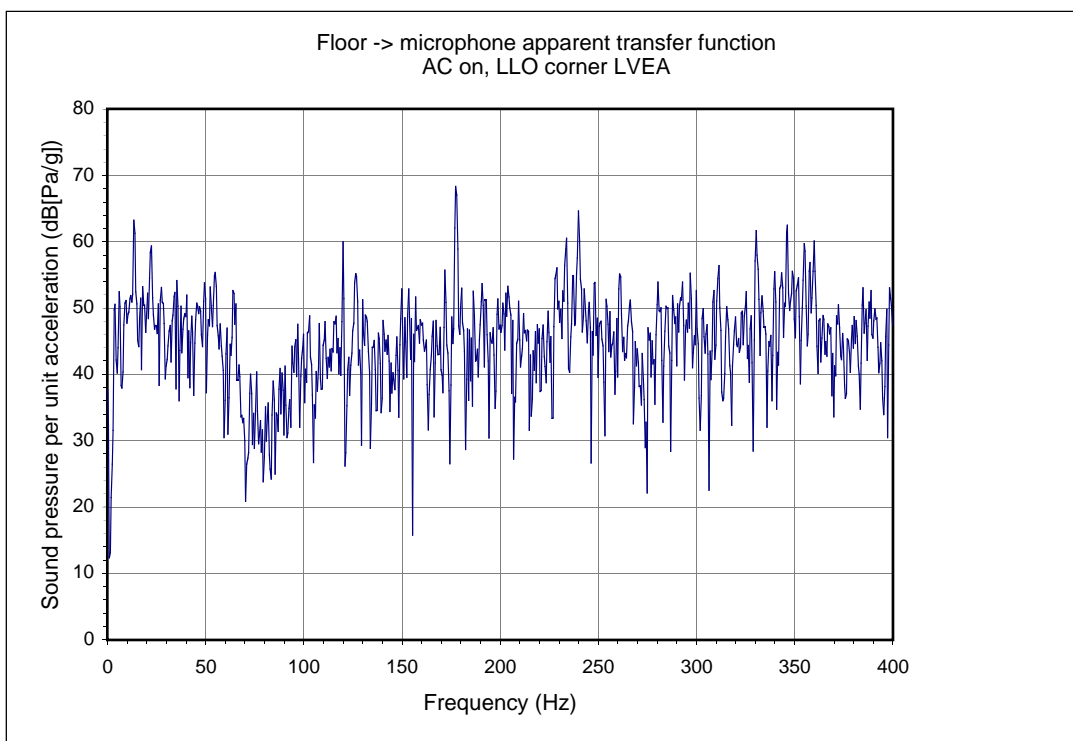


Figure 12: Apparent cross-spectral transfer function between floor acceleration and sound. Compare with the ratio between cyan and green curves in Figure 11.

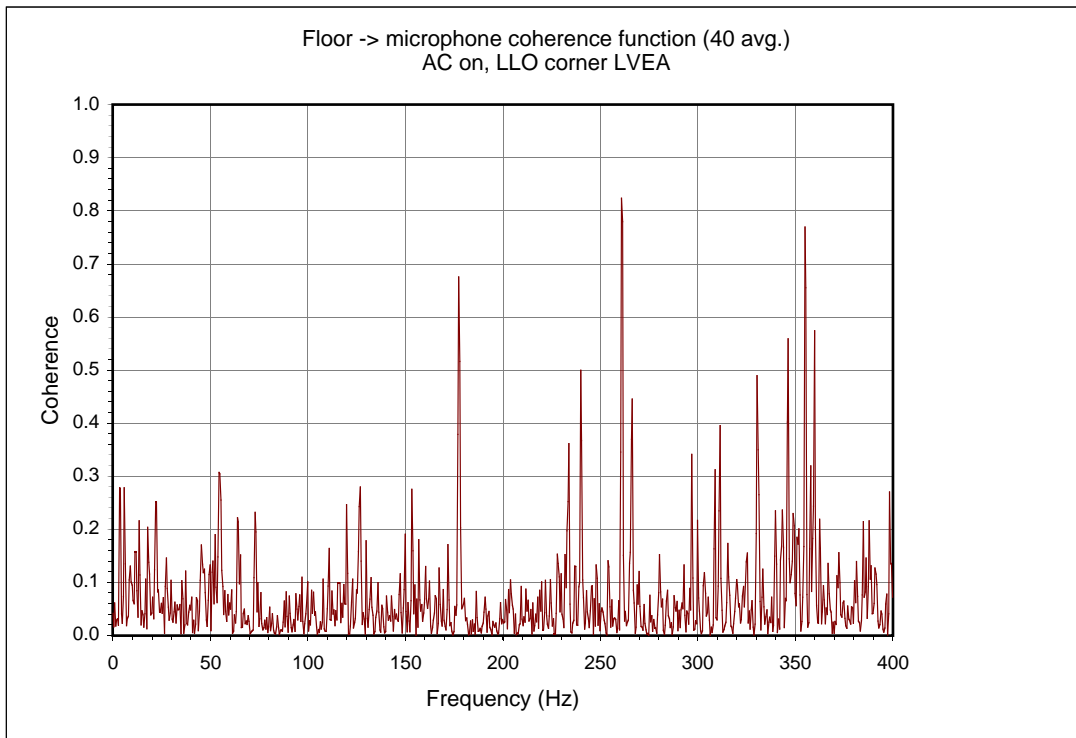


Figure 13: Coherence function between floor acceleration and sound. Based on 40 2-second samples, with HVAC operating (same data as Figures 11 and 12).

5 DISCUSSION AND RECOMMENDATIONS

To be updated following data conference with CAA, scheduled for 1/7/99.

- 5.0.1. Seal openings to mechanical rooms & test transmission before/after**
- 5.0.2. Extend measurements to low frequencies (< 1 Hz) using seismometers**
- 5.0.3. Investigate cryopump bubbling noise**
- 5.0.4. Install weather stations & correlate vibration with wind & rainfall**
- 5.0.5. Evaluate stationarity of HVAC noise; correlate with fan cycles**
- 5.0.6. Map & quantify acoustic/vibration transfer function**
- 5.0.7. Determine correlation length of acoustic excitations in LVEA**
- 5.0.8. Reduce CW circulation and HVAC fan noise in VEA/LVEA**
- 5.0.9. Evaluate contribution of wastewater treatment plant at LVEA**